Registration of Images With N-Fold Dihedral Blur

Matteo Pedone, Jan Flusser, *Senior Member, IEEE*, and Janne Heikkilä, *Senior Member, IEEE*

***Abstract*— In this paper, we extend our recent registration method designed specifically for registering blurred images. The original method works for unknown blurs, assuming the blurring point-spread function (PSF) exhibits an N-fold rotational symmetry. Here, we also generalize the theory to the case of dihedrally symmetric blurs, which are produced by the PSFs having both rotational and axial symmetries. Such kind of blurs are often found in unfocused images acquired by digital cameras, as in out-of-focus shots the PSF typically mimics the shape of the shutter aperture. This makes our registration algorithm particularly well-suited in applications where blurred image registration must be used as a preprocess step of an image fusion algorithm, and where common registration methods fail, due to the amount of blur. We demonstrate that the proposed method leads to an improvement of the registration performance, and we show its applicability to real images by providing successful examples of blurred image registration followed by depth-of-field extension and multichannel blind deconvolution.**

***Index Terms*— Image registration, blurred images, N-fold rotational symmetry, dihedral symmetry, phase correlation.**

I. Introduction

IMAGE registration, a process of spatial overlaying two or more images of the same scene, is one of the most important tasks in image pre-processing. As such, it has received considerable attention and hundreds of papers have been published on this subject (see [1] for a survey). Since there obviously does not exist any unique always-optimal approach, many authors have proposed specific registration methods for particular application areas, for particular kind of data and/or for a certain class of between-image deformations.

In many cases, the images to be registered (or at least one of them) are blurred (Fig. 1). The blur may originate from camera shake and/or wrong focus, scene motion, atmospheric turbulence, sensor imperfection, low sampling density and other factors. The demand for blurred image registration comes namely from applications, where a short sequence of low-quality images is used to produce a single sharp high-resolution output (multichannel image deconvolution, super-resolution, image fusion, among others).

Manuscript received October 29, 2013; revised February 10, 2014 and November 18, 2014; accepted December 31, 2014. Date of publication January 12, 2015; date of current version January 30, 2015. This work was supported in part by the Czech Science Foundation under Grant GA13-29225S and Grant GA15-16928S and in part by the Academy of Finland under Grant 259431. The associate editor coordinating the review of this manuscript and approving it for publication was Dr. Chun-Shien Lu.

M. Pedone and J. Heikkilä are with the Center for Machine Vision Research, Department of Computer Science and Engineering, University of Oulu, Oulu FI-90014, Finland (e-mail: matped@ee.oulu.fi; jth@ee.oulu.fi).

J. Flusser is with the Institute of Information Theory and Automation, Czech Academy of Sciences, Prague 182 08, Czech Republic (e-mail: flusser@utia.cas.cz).

Color versions of one or more of the figures in this paper are available online at http://ieeexplore.ieee.org.

Digital Object Identifier 10.1109/TIP.2015.2390977

Fig. 1. Two images to be registered – the reference image *(left)* and the blurred sensed image *(right)*. The blurring PSF is shown in the upper right corner.

Registration of blurred images requires special methods because general registration methods usually do not perform well on blurred images. Several landmark-based blur-invariant registration methods appeared during the last 15 years [2]–[7]. They can in principle handle affine distortions or even distortions beyond the global linear model but they are sensitive to noise and often perform slowly because they consist of detection of the control point candidates and their subsequent matching in the feature space.

Some authors realized that simple and much faster global techniques can perform surprisingly well. When registering short time sequences, the input images differ mostly by a shift (and perhaps by a small rotation) and their overlap can be 60-80% or even more. So, the challenge is to estimate this shift in case the inputs are (possibly heavily) blurred. Such global techniques were motivated by the well-known approach of phase correlation [8] and tried to make this traditional method insensitive or even invariant to image blur. This idea was originally proposed by Ojansivu et al. [9], who realized that the square of the normalized cross-power spectrum is not influenced by the image blur assuming the blurring point-spread function (PSF) is centrosymmetric. The same method was later rediscovered by Tang et al. [10] in connection with X-ray image registration. Most recently, Pedone et al. [11] presented the theory of image projection operators and showed how these projections can be used for developing a registration method which is invariant to arbitrary image blur provided that the blurring kernels exhibits the so-called N-fold rotational symmetry. This was a novel idea because most DSLR and compact cameras have the out-of-focus PSF of this kind, due to the polygonal aperture formed by diaphragm blades (see Fig. 2). Pedone et al. also explained in [11] that it is desirable to use such version of the method which was developed particularly for the type of symmetry that the ground-truth PSF actually shows. Even if their method could work for some other settings as well, we always lose

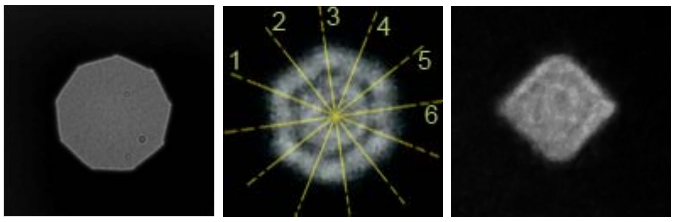

Fig. 2. The PSF's of three common compact cameras. Nine-fold rotational symmetry *(left)*, six-fold dihedral symmetry with symmetry axes superimposed, obtained from a Panasonic Lumix DMC-LX3 *(middle)*, and four-fold dihedral symmetry, obtained from a Panasonic HC-V700 *(right)*.

a part of useful information when the assumed and real PSF symmetries are not the same.

Our recent analysis of the out-of-focus PSF's of several common cameras has shown that they not only have N-fold rotational symmetry but they mostly also have *axial* symmetry with respect to N axes; such "combined" symmetry is in mathematics called *dihedral symmetry*. In Fig. 2 we can see the PSF's of three cameras obtained by taking a photo of a single bright point. The shape of the PSF is sometimes apparent even in real scenes, see Fig. 11 top-right for an example.

Axial symmetry was not considered in [11] at all, although it carries additional information about the PSF. In this paper, we extend the theory and the registration method originally proposed in [11] to the blurs with dihedral symmetry by defining new dihedral projection operators. We show this extension has a practical impact because we essentially utilize more information about the PSF compared to the pure N-fold rotational assumption, which increases the registration performance particularly in case of noisy images and of a low image overlap.

II. Recalling the Original Method

The method introduced in [11] assumes that the sensed image g is a blurred and shifted version of the reference image f

$$g(\mathbf{x}) = (f * h)(\mathbf{x} - \Delta), \tag{1}$$

where the convolution kernel h stands for the PSF of the imaging system, which is responsible for blurring, and Δ is an unknown between-image shift to be recovered by the registration.

The core idea is not to register the images f and g directly but rather to eliminate the impact of the convolution kernel by constructing new blur-invariants, and register these blur-invariant representations of the images by phase correlation.

The crucial assumption on the PSF made in [11] is its N-fold rotational symmetry, i.e.

$$h(r, \theta) = h(r, \theta + 2\pi j/N) \qquad j = 1, \ldots, N.$$

The blurring is eliminated by using projection operators. Projection operators are defined in Fourier domain as

$$K_j^{(f)}(\mathbf{u}) = \frac{F(\mathbf{u})}{F(R_j\mathbf{u})} \quad j = 1, \ldots, N \tag{2}$$

where $F(\mathbf{u}) \stackrel{def}{=} \mathcal{F}\{f\}(\mathbf{u})$ is the Fourier transform of $f(\mathbf{x})$, and $R_j\mathbf{u}$ means a rotation of the frequency coordinates by the angle $2\pi j/N$. These operators do not change if the image is blurred by an arbitrary N-fold symmetric PSF and preserve their magnitude if the image is translated in the spatial domain (see [11] for the proofs). Hence, one can apply a "modified phase correlation", where the normalized cross-power spectrum is not calculated directly from the Fourier transforms F and G, but rather from their corresponding projections $K_j^{(f)}$ and $K_j^{(g)}$ as

$$C_j = \frac{K_j^{(f)} K_j^{(g)*}}{|K_j^{(f)}||K_j^{(g)}|} = \frac{K_j^{(f)} K_j^{(g)*}}{|K_j^{(f)}|^2} = \\ = \frac{K_j^{(f)}}{K_j^{(f(\mathbf{x}-\Delta))}} = e^{-i\mathbf{u}\cdot(\mathrm{R}_j^{\mathrm{T}}\Delta - \Delta)}. \tag{3}$$

Hence, each $\mathcal{F}^{-1}\{C_j\}$ yields a delta function located at intervals of $2\pi j/N$ radians along a circle centered at $\mathbf{x} = -\Delta$ and passing through the origin (see Fig. 3a). As soon as these delta-peaks have been detected, they are fitted by a circle. The center of such circle directly represents the shift vector Δ between the reference and sensed images.

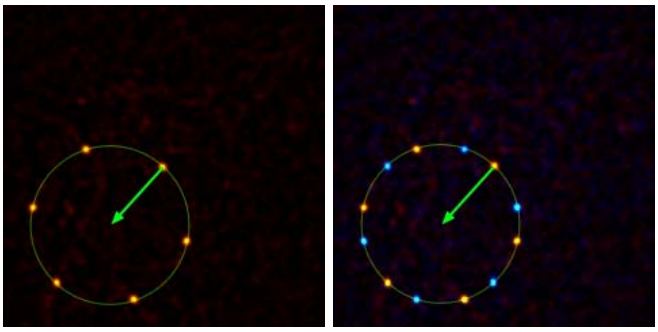

(a) (b)

Fig. 3. Registration of the two images in Fig. 1. Six spectral peaks produced by the method from [11] *(left)*, and twelve spectral peaks produced by the proposed dihedral method *(right)*. The shift is given by the center of the circle.

III. Blur Invariant Operators

We have seen that the construction of the blur-invariant registration method is possible thanks to the N-fold symmetry of the PSF. Any extension and generalization to other types of PSF's must be based on studying their symmetric properties, which consequently should enable to find proper projection operators and proceed analogously to [11]. Symmetry in 2D has been traditionally studied in group theory. It is well known that in 2D there exist only two kinds of symmetry groups which are relevant to our problem: cyclic groups C_N that contain N-fold rotational symmetry and dihedral groups D_N that contain rotation *and* reflection symmetry. The relationship between these two symmetries is that if a function shows N-fold rotational symmetry, then it may only have either none or N symmetry axes. On the other hand, having N symmetry axes immediately implies N-fold rotational symmetry. Therefore, $D_N \subsetneqq C_N$ for finite N, and $D_\infty = C_\infty$.

Hence, it is meaningful to deal with registration of images with PSF's having dihedral symmetry, for two reasons – such situation appears frequently in practice, and at the same time

is mathematically tractable. Since the group C_N has only one generator (elementary rotation R_1), while D_N has two generators (elementary rotation and reflection), we may expect that in case of dihedral symmetric PSF there exist two times more projections analogous to (2) and the method will double the number of delta-peaks, which should further lead to a more robust fit, especially in such cases when the localization of the peaks is difficult due to noise.

The rotation operator R_j was already mentioned in the previous section. The reflection operator S is given as

$$S(\mathbf{x}) = \begin{bmatrix} \cos 2\alpha & \sin 2\alpha \\ \sin 2\alpha & -\cos 2\alpha \end{bmatrix} \begin{bmatrix} x \\ y \end{bmatrix}$$

where α is the angle between the reflection line (symmetry axis) and the horizontal axis. Any operator D from D_N can be expressed as a certain finite concatenation of the generators R_1 and S.

Now we can construct quantities in Fourier domain, which are invariant w.r.t. a convolution with arbitrary dihedral PSF. Any ratio of the form

$$\frac{\mathcal{F}\{f\}}{\mathcal{F}\{Df\}}$$

where D is an arbitrary operator from D_N has such property. It is sufficient to prove that for $D = R_1$ and $D = S$, which is easy:

$$\frac{\mathcal{F}\{f * h\}}{R_1\mathcal{F}\{f * h\}} = \frac{F \cdot H}{R_1 F \cdot R_1 H} = \frac{\mathcal{F}\{f\}}{\mathcal{F}\{R_1 f\}}, \tag{4}$$

$$\frac{\mathcal{F}\{f * h\}}{S\mathcal{F}\{f * h\}} = \frac{F \cdot H}{SF \cdot SH} = \frac{\mathcal{F}\{f\}}{\mathcal{F}\{Sf\}}. \tag{5}$$

In (4) and (5) we used the commutativity between D and the Fourier transform along with the fact that $DH = H$ because of dihedral symmetry of H (which is guaranteed thanks to the dihedral symmetry of h).

For our purpose we use the following invariants to dihedral blur

$$\mathcal{K}_j = \frac{\mathcal{F}\{f\}}{\mathcal{F}\left\{R_j f\right\}}, \tag{6}$$

$$\mathcal{L}_j = \frac{\mathcal{F}\{f\}}{\mathcal{F}\left\{R_j S f\right\}}. \tag{7}$$

for $j = 1, \ldots, N$. Note that the invariants $\mathcal{K}_j$ are the same as those introduced in [11] (which is in accordance with the fact that D_N is a subgroup of C_N), while the invariants $\mathcal{L}_j$ are new. Now we have $2N$ invariants, which is a redundant number, but similarly to [11] we will work with all of them to reach high robustness.

IV. Image Registration Algorithm

The invariants introduced in the previous section will be now used to design a robust blur-invariant registration method. The main idea is that we may consider the invariants to be Fourier transforms of hypothetical non-blurred images, which can be registered by phase correlation.

We calculate the normalized cross-power spectra

$$C_j = \frac{\mathcal{K}_j^{(f)} \mathcal{K}_j^{(g)*}}{\left|\mathcal{K}_j^{(f)} \mathcal{K}_j^{(g)}\right|} \tag{8}$$

and

$$B_j = \frac{\mathcal{L}_j^{(f)} \mathcal{L}_j^{(g)*}}{\left|\mathcal{L}_j^{(f)} \mathcal{L}_j^{(g)}\right|} \tag{9}$$

for every $j = 1, \ldots, N$. It was proved in [11] that the inverse Fourier transform of C_j yields a shifted delta function

$$\mathcal{F}^{-1}\left\{C_j\right\}(\mathbf{x}) = \delta\left(\mathbf{x} + \Delta - R_{N-j}\Delta\right). \tag{10}$$

Let us investigate the behavior of B_j. Using the properties of the invariants we get

$$B_j = \frac{F}{R_j SF} \frac{(R_j SF)(R_j SH)}{FH e^{-i\mathbf{u}\cdot\Delta}} e^{-i(R_j S\mathbf{u})\cdot\Delta}. \tag{11}$$

Due to the dihedral symmetry of H we have $H = R_j SH$. Using the identity

$$(R_j S\mathbf{u}) \cdot \Delta = \mathbf{u} \cdot (SR_{N-j}\Delta)$$

we obtain

$$B_j(\mathbf{u}) = e^{i\mathbf{u}\cdot\left(\Delta - SR_{N-j}\Delta\right)}. \tag{12}$$

Taking the inverse Fourier transform of B_j we get

$$\mathcal{F}^{-1}\left\{B_j\right\}(\mathbf{x}) = \delta\left(\mathbf{x} + \Delta - SR_{N-j}\Delta\right). \tag{13}$$

Hence, we can see that $\mathcal{F}^{-1}\left\{B_j\right\}$ is also a shifted delta function. All peaks produced by both $\mathcal{F}^{-1}\left\{C_j\right\}$ and $\mathcal{F}^{-1}\left\{B_j\right\}$ lie on the same circle, the center of which is at $-\Delta$ (see Fig. 3b).

The registration is completed by fitting a circle over all the delta-peaks. The fitting algorithm minimizes the ℓ_p error and is exactly the same as that in [11], including the choice of an appropriate p. As in [11], we use $p = 0.2$ in our experiments. The only difference is that here we fit a double number of peaks ($2N$ instead of N), which generally leads to an improvement, since we experimentally observed that the probability distribution of localization error is the same as the one we reported in [11] for all peaks, both N-fold and dihedral peaks. From this it is clear that adding new peaks cannot worsen the fit. This is the main advantage of the presented method.

The distribution of the peaks along the circle is generally *not* uniform, although within each of the two sets of peaks the peaks are equally spaced. The distance between the peaks from the first and the second set depends not only on N but also on the angle between the shift vector and the symmetry axis of the PSF. In the limit case, the two sets of peaks coincide. We should also mention that while the peaks coming from $\mathcal{F}^{-1}\left\{C_j\right\}$ could lie anywhere in the plane depending solely on the shift vector, the positions of the peaks generated by $\mathcal{F}^{-1}\left\{B_j\right\}$ are constrained to lie on straight lines passing through the origin. In fact, if we suppose the operator $S = S_{\mathbf{a}}$ reflects across a chosen vector $\mathbf{a}$, and we consider the half-angle rotation operator $R_{i/2}$, it can be verified that $R_i S_{\mathbf{a}} = S_{R_{i/2}\mathbf{a}}$, thus, for any $i = 1, \ldots, N$:

$$SR_i\Delta - \Delta = 2\mathrm{Proj}_{R_{i/2}\mathbf{a}_\perp}(\Delta) \tag{14}$$

where $\mathbf{a}_\perp$ is the vector $\mathbf{a}$ rotated by 90°, and the operator Proj projects orthogonally Δ onto rotated versions of $\mathbf{a}_\perp$. This observation can be used as a hint which simplifies

Algorithm 1 Pseudocode for Dihedral Blur Invariant Phase Correlation

INPUT: images f, g such that satisfy Eq. (1)
$N :=$ number of N-fold symmetry of the PSF
$\alpha :=$ orientation of the symmetry axis of the PSF
OUTPUT: translational shift $\mathbf{\Delta} \in \mathbb{R}^2$ between f and g

1: **for** $j = 1$ to N **do**
2: calculate $\mathcal{K}_j^{(f)}$ and $\mathcal{K}_j^{(g)}$ according to Eq. (6)
3: calculate C_j according to Eq. (8)
4: $peak[j] \leftarrow \arg_{\mathbf{x}} \max \mathcal{F}^{-1}\{C_j\}(\mathbf{x})$
5: calculate $\mathcal{L}_j^{(f)}$ and $\mathcal{L}_j^{(g)}$ according to Eq. (7)
6: calculate B_j using α according to Eq. (9)
7: $peak[j+N] \leftarrow \arg_{\mathbf{x}} \max \mathcal{F}^{-1}\{B_j\}(\mathbf{x})$
8: **end for**
9: $d[j] :=$ Euclidean distance between $peak[j]$ and candidate circle
10: $\Theta :=$ circle minimizing $\ell_{0.2}-$norm of vector $d[j]$
11: $\mathbf{\Delta} \leftarrow$ center of circle Θ

the localization of the peaks. The pseudocode in Algorithm 1 summarizes the steps of a basic version of the registration algorithm described in this section.

Without any modification, the above theory is valid also for registering two images which are both blurred (possibly differently, but with the PSF's of the same kind of symmetry). The model (1) is then generalized into the form

$$(o * h_1)(\mathbf{x}) = (o * h_2)(\mathbf{x} - \Delta), \tag{15}$$

where $o(\mathbf{x})$ is the original unobservable scene. This formulation is common in multichannel restoration and in image fusion.

V. Estimation of the Symmetry Axis

While N is fixed for the particular camera and mostly known in advance, the orientation of the symmetry axis of the PSF depends on the camera rotation and also changes as the aperture opens/closes, so it may not be known *a priori*. In some cases the axis orientation can be estimated directly from the bright patterns in the blurred image, but in other cases a general estimation algorithm is required. We propose here a simple algorithm to estimate the orientation of one of the symmetry axes of a PSF having dihedral symmetry.

Provided (1) holds, the Fourier Shift Theorem guarantees $|G| = |F||H|$, and we can in principle estimate $|H|$ by calculating the ratio $|G|/|F|$. However, in order to estimate $|H|$ more robustly we rather calculate the ratio of the N-fold rotational projections of $|G|$ and $|F|$, that is:

$$|H| = \frac{\sum_{i=1}^{N} R_i |G|}{\sum_{i=1}^{N} R_i |F|}. \tag{16}$$

The above calculation is justified by the fact that the projections in (16) remove all parts of the spectra which are not N-fold symmetric, thus no information of $|H|$ is discarded [11]. The reader should in fact recognize that the quantities at the numerator and denominator of (16) extract the N-fold symmetric parts of respectively $|G|$ and $|F|$. Furthermore, notice that the N-fold rotational projections are averages of rotated versions of the spectra, thus they also reduce the variance of statistically independent noise. $|H|$ has the same kind of dihedral symmetry as h with the same axes orientation. Let us denote the angle between the horizontal axis and the symmetry axis of $|H|$ by α. Let $|H'|$ be a mirrored version of $|H|$ across the horizontal axis. Hence, the symmetry axis of $|H'|$ is oriented at the angle $-\alpha$, and, thanks to the dihedral symmetry, we have

$$\left| H'\left(r, \theta - 2\alpha - \frac{2\pi}{N}k\right)\right| = |H(r,\theta)| \tag{17}$$

for any integer k. Thus, the cross-correlation in polar coordinates in the angular direction

$$X_H(\theta) = \int_0^{2\pi} \int_0^{+\infty} |H(r,\phi)| \left|H'(r,\phi-\theta)\right| r dr d\phi \tag{18}$$

produces N peaks located at $\theta = 2\alpha + \frac{2\pi}{N}k$, where $k = 0, \ldots, N-1$. We estimate α as

$$\alpha_{est} = \frac{1}{2} \arg_\theta \max X_H(\theta) \tag{19}$$

(see Fig. 4 for an illustration of the procedure).

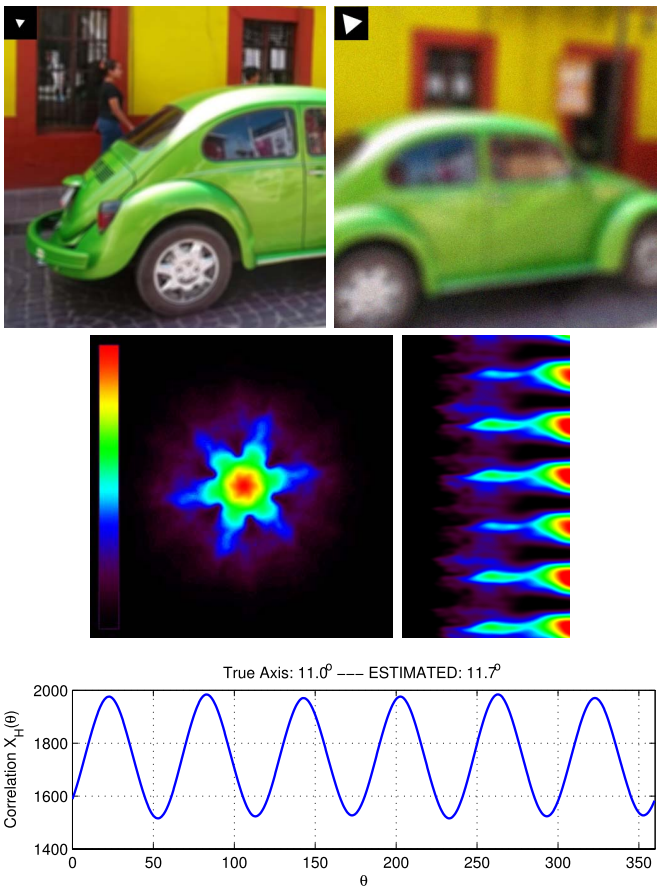

Fig. 4. Two blurred images with 50% overlap. The PSF's have 3-fold dihedral symmetry and the same symmetry axes. The second image was corrupted by additive Gaussian noise with $\sigma = 10$ *(top)*. The resulting $|H|$ from (16) and its representation in polar coordinates *(middle)*. The cross-correlation $X_H(\theta)$ shows that the estimation of the symmetry axis is relatively accurate *(bottom)*.

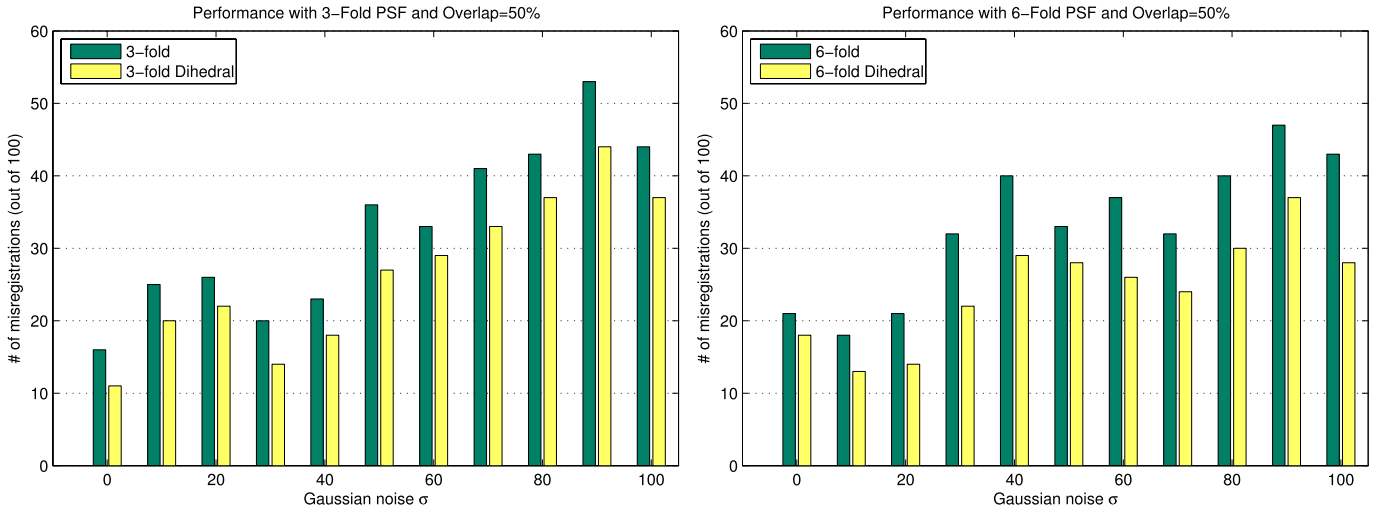

Fig. 5. The number of misregistrations for different levels of noise when the true PSF had 3-fold dihedral symmetry *(left)*, and 6-fold dihedral symmetry *(right)*. The green (dark) bars show the performance of the method from [11], the yellow (light) bars come from the proposed algorithm.

The above procedure is correct only for even N. If N is odd, then the symmetry of $|H|$ is actually $2N$-fold, because the magnitude spectrum of any real signal is always centrally symmetric, i.e. 2-fold, thus any odd-fold symmetry in space-domain gets doubled in the magnitude spectrum. In the example of Fig. 4 it is evident that the magnitude spectrum of a 3-fold PSF is actually 6-fold. For this reason, when the described algorithm detects a peak, we cannot decide directly if α_{est} is a correct estimate for α, or if it is an estimate for $\alpha + \pi/2N$. In order to resolve this ambiguity we re-evaluate twice (16) and (18) with $g_1(\mathbf{x}) = (g * p_1)(\mathbf{x})$, and $g_2(\mathbf{x}) = (g * p_2)(\mathbf{x})$ used in place of g. The functions p_1, p_2 are arbitrarily shaped PSF's having exact N-fold dihedral symmetry, with symmetry axes respectively equal to α_{est} and $\alpha_{est} + \frac{\pi}{2N}$. If $\alpha \neq \alpha_{est}$ then the "composite" PSF $s_1(\mathbf{x}) = (h * p_1)(\mathbf{x})$ will have only N-fold rotational symmetry, but not dihedral symmetry, so identity (17) in general will not hold for $|S_1|$. On the other hand, if $\alpha = \alpha_{est} + \frac{\pi}{2N}$, then $s_2(\mathbf{x}) = (h * p_2)(\mathbf{x})$ has dihedral symmetry; identity (17) now holds for $|S_2|$, and the correlation peaks of X_{S_2} are higher than those obtained from X_{S_1}. The last observation is used as a criterion to select the correct estimate for α. If the peaks of X_{S_1} and X_{S_2} are comparable, we consider $2N$ to be the true fold number and both α_{est} and $\alpha_{est} + \frac{\pi}{2N}$ are correct orientations of the symmetry axes.

The described estimation procedure works even if both images are blurred, provided that both PSF's have the same kind of symmetry and the same orientation. In fact, if f and g are respectively blurred by two different PSF's h_1 and h_2, then we have to replace $|G|$ and $|F|$ in (16) with respectively $|F||H_1|$ and $|F||H_2|$. But since H_1 and H_2 have the same symmetry and the same axis orientation, also $|H_1|/|H_2|$ will have the same symmetry and same orientation, and so the whole quantity calculated in (16) (Fig. 4, middle).

VI. Estimation of N

The parameter N of the blur PSF is generally determined by the mechanical design of the shutter, and it normally coincides with the number of shutter blades, thus it remains fixed for a specific device. N is often known in advance, or at least, easy to obtain by visually inspecting either the shutter, or a blurred image where the shape of the PSF manifests itself (see for instance Fig. 11, top right). However, in some cases, the user might need to estimate N directly from the blurred image. Most of the techniques seen in Section V can be re-used to derive a simple algorithm for the estimation of N. In fact, assuming (1) holds, it is sufficient to estimate the magnitude of the PSF by:

$$|H| = \frac{|G|}{|F|} \tag{20}$$

and then calculate the polar cross-correlation $X_H(\theta)$ as in Eq. (18). An estimate for N can be simply obtained by counting the number of peaks in the plot of $X_H(\theta)$ (see Fig. 4, bottom), or more robustly by detecting its fundamental frequency from the magnitude of the Fourier series expansion

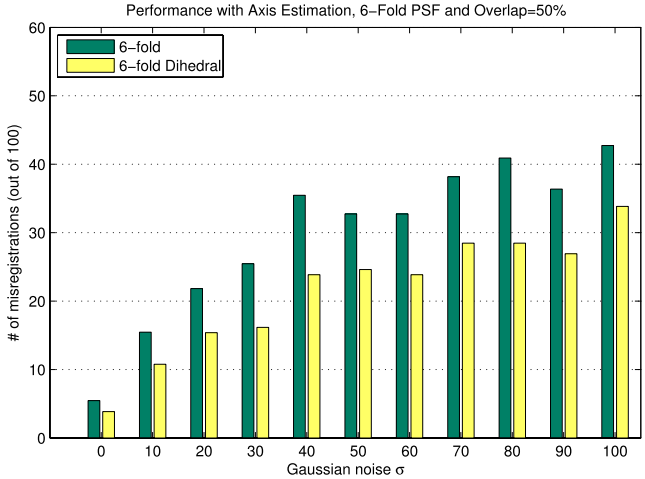

Fig. 6. Percentage of misregistrations for different levels of noise when using the axis estimation algorithm described in Section V. The true PSF had 6-fold dihedral symmetry.

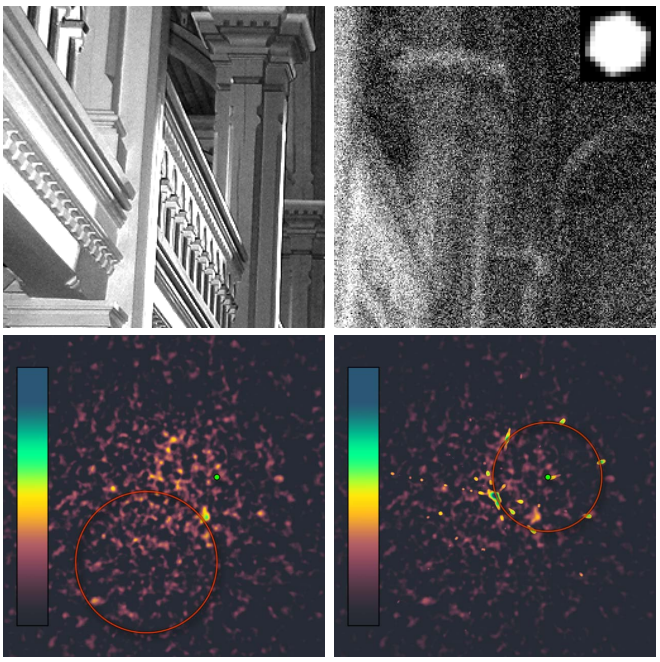

Fig. 7. An image pair where one is heavily blurred with a PSF of $N = 6$ and noisy ($\sigma = 40$) *(top)*. The spectral patterns of $\mathcal{F}^{-1}\{C_j\}$: only one correct peak was found, the circle fit was wrong and the registration failed. The true shift is represented by the green dot *(bottom left)*. Adding the six extra spectral patterns $\mathcal{F}^{-1}\{B_j\}$ yielded a correct registration *(bottom right)*.

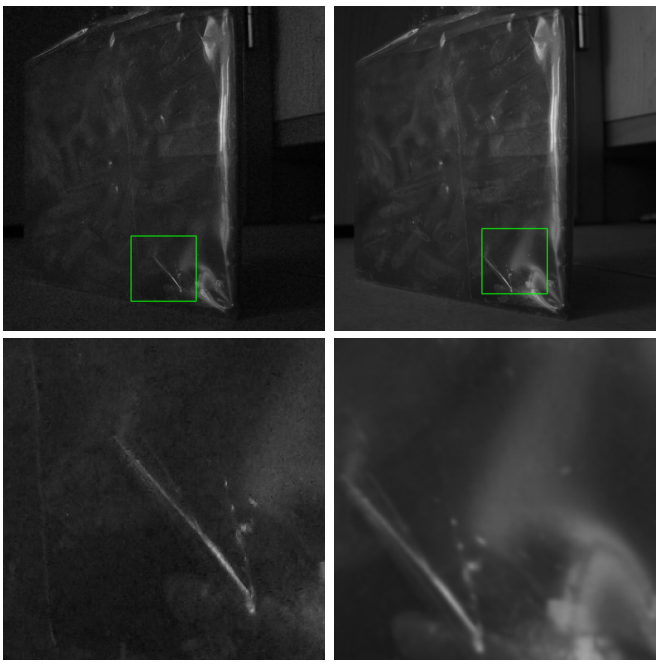

Fig. 8. Two images used in the experiment with real noise. The noise on the left image is caused by a short exposure time *(top row)*. Magnified versions of the two rectangular patches enclosed in the green boxes. The patches to be registered have size 256×256 pixels, and their overlap is 50% *(bottom row)*. One hundred of this kind of image pairs were registered with our algorithm.

of X_H, i.e.:

$$N_{est} = \arg_{k \geq 2} \max |\mathcal{F}\{X_H\}(k)| \tag{21}$$

where the frequency k is always an integer. The reader might have noticed that in (20) we did not use the projection

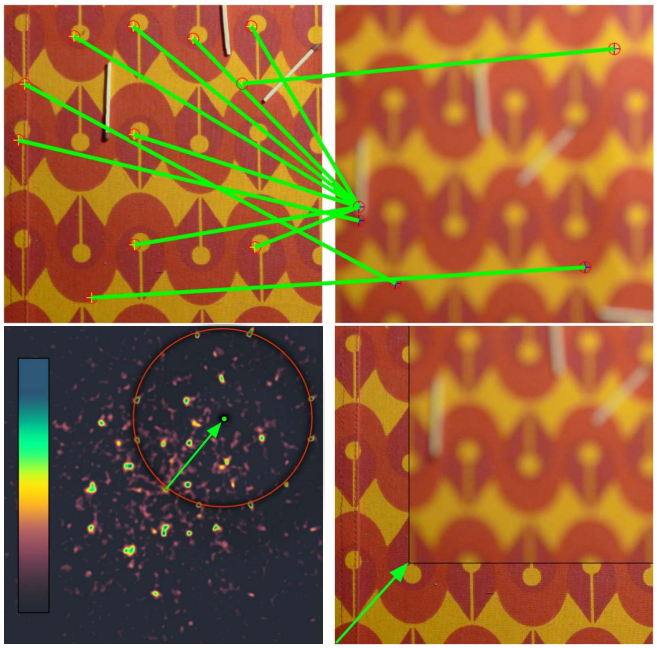

Fig. 9. Two images acquired by a hand-held camera with different focus settings and shift. Matched SIFT features are connected by green lines: SIFT-based registration failed *(top row)*. The sum of the spectral patterns $\mathcal{F}^{-1}\{C_j\}$ and $\mathcal{F}^{-1}\{B_j\}$. The green arrow represents the estimated shift. The spectra visibly exhibit some periodicity because of the repeating structures in the images *(bottom left)*. The registration result by the proposed method. The registered blurred image is overlaid over the reference one, which enables to check the accuracy visually *(bottom right)*.

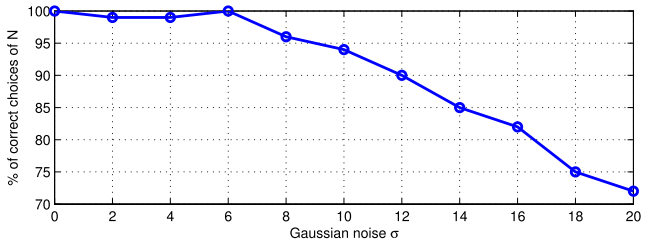

Fig. 10. Percentage of correct choices of N for different levels of noise when using the estimation algorithm described in Section VI.

operators as we did in (16), since N is now unknown. This makes the estimation of N potentially more vulnerable to high levels of noise. However, as we will see from the experiments in Section VII, the estimation of N is relatively accurate even when a moderate amount of noise is present in the images. Another important observation is that, due to the 2-fold symmetry of the magnitude spectrum $|H|$, the estimation procedure described above is correct only for even N. In fact, when N is odd, (21) yields $N_{est} = 2N$, and one cannot immediately decide whether the true N is given directly by N_{est} or by $N_{est}/2$. We resolve this ambiguity by adopting the same strategy explained in the last part of Section V.

VII. Experiments

We compared the presented method with the N-fold phase correlation approach described in [11]. We did not present here a comparison to other state-of-the-art methods because such a comparison was already done for N-fold phase correlation

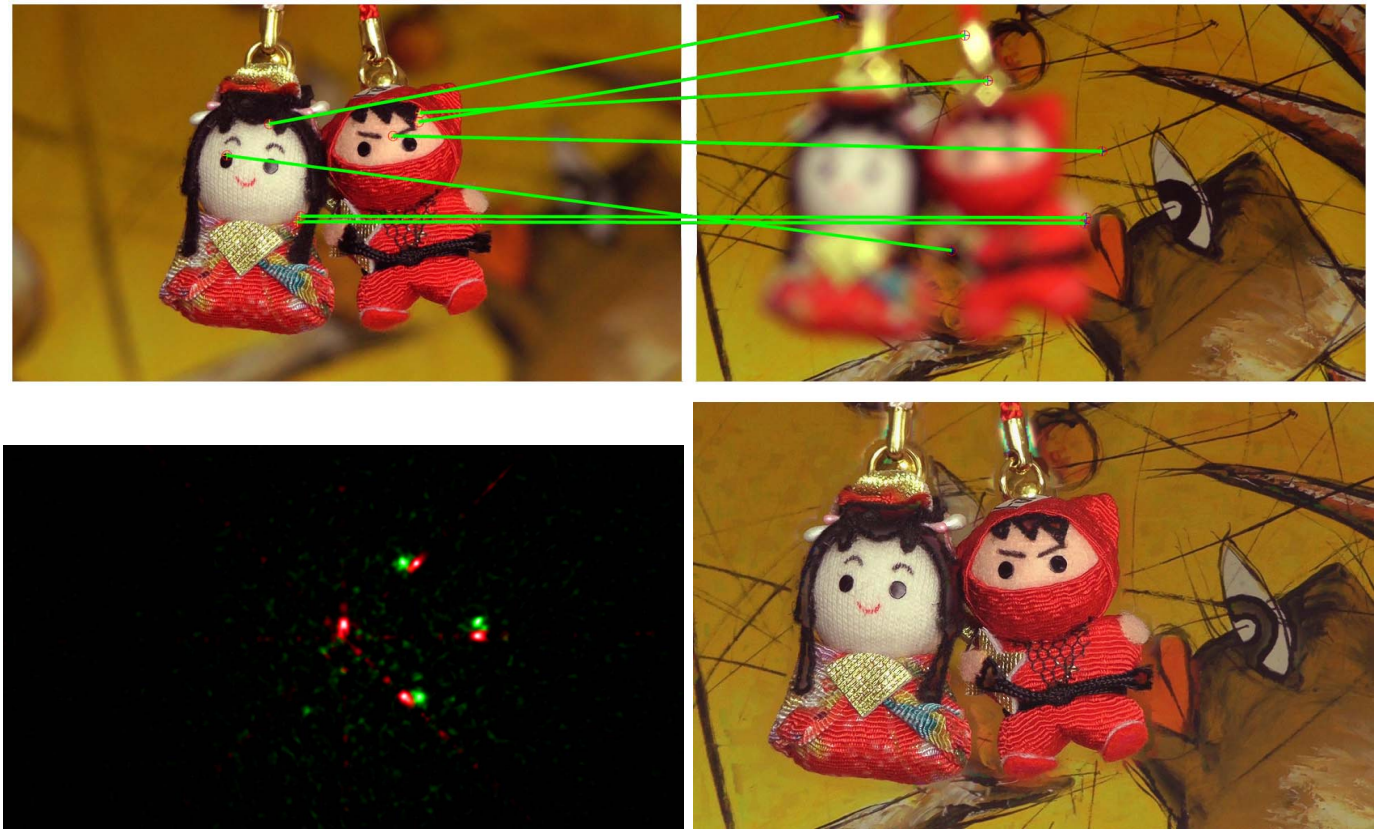

Fig. 11. Two frames from a video sequence taken with different focus settings. SIFT-based registration failed. The matched features are connected by green lines *(top)*. The PSF of a dihedral shape ($N = 4$) is clearly visible in the second frame due to the bright points in the foreground which are out of focus *(top right)*. Spectral patterns, where the red part represents the dihedral peaks $\mathcal{F}^{-1}\{B_j\}$ *(bottom left)*. Result of multifocus fusion *(bottom right)*.

in [11] and can be easily repeated with analogous results. The same is true for experimenting with various image overlaps and for the robustness with respect to an incorrect choice of N. To avoid redundancy, we concentrated on studying differences between the proposed method and the N-fold phase correlation method [11].

The main difference in performance of both methods appears when registering noisy images with low overlap, as is demonstrated by the following experiment. We took ten 4-megapixels images with a consumer camera and converted them to grayscale for simplicity (the algorithm works with color images as well, treating them band by band). For each of these, a corrupted version was artificially created by blurring the original image with a PSF of 31×31 pixels, a specified degree N of dihedral symmetry, and random but known symmetry axis. In addition to the blur, each image was corrupted by additive Gaussian white noise. The image intensity values were in the range $[0, 255]$, and the noise standard deviations σ used in the experiments were 0, 10, 20, 30, 40, 50, 60, 70, 80, 90, and 100, respectively. From each of these images, ten pairs of square patches of the size 256×256 pixels and a percentage of 50% of overlapping area were extracted at random locations, one from the sharp image, and the other one from its blurred and noisy version, giving a total number of 1100 image pairs to be registered (100 pairs on each noise level). The new dihedral phase correlation and the N-fold phase correlation [11] were used to register them. We evaluated the performance of the methods by counting the number of misregistrations, where any registration error greater than 1 pixel in terms of Euclidean distance is considered as a misregistration. The choice of this criterion has been justified in [11]. The results are shown in Fig. 5 for $N = 3$ and $N = 6$. Other choices of N produced analogous results. The average increase in performance observed using the proposed method was approximately 11%. Although the improvement is observable on each noise level (including the noise-free case), it increases as the noise variance increases.

When using the algorithm for symmetry axis estimation described in Section V, the resulting plots looked analogous to the ones in Fig. 5 although the average increase in performance was 8% (Fig. 6). When we did not apply any axis estimation method and "estimated" the axis orientation randomly, the method performance converged to that of the N-fold method. This behavior is to be expected because, as we demonstrated in [11], our algorithm for the circle-fit can easily tolerate slightly more than 50% of outliers.

Fig. 7 shows an example where the N-fold phase correlation failed and a correct registration could only be obtained by utilizing the information coming from the extra peaks of dihedral phase correlation.

An analogous experiment to the one described above was run for 100 pairs of real images taken in low-light conditions,

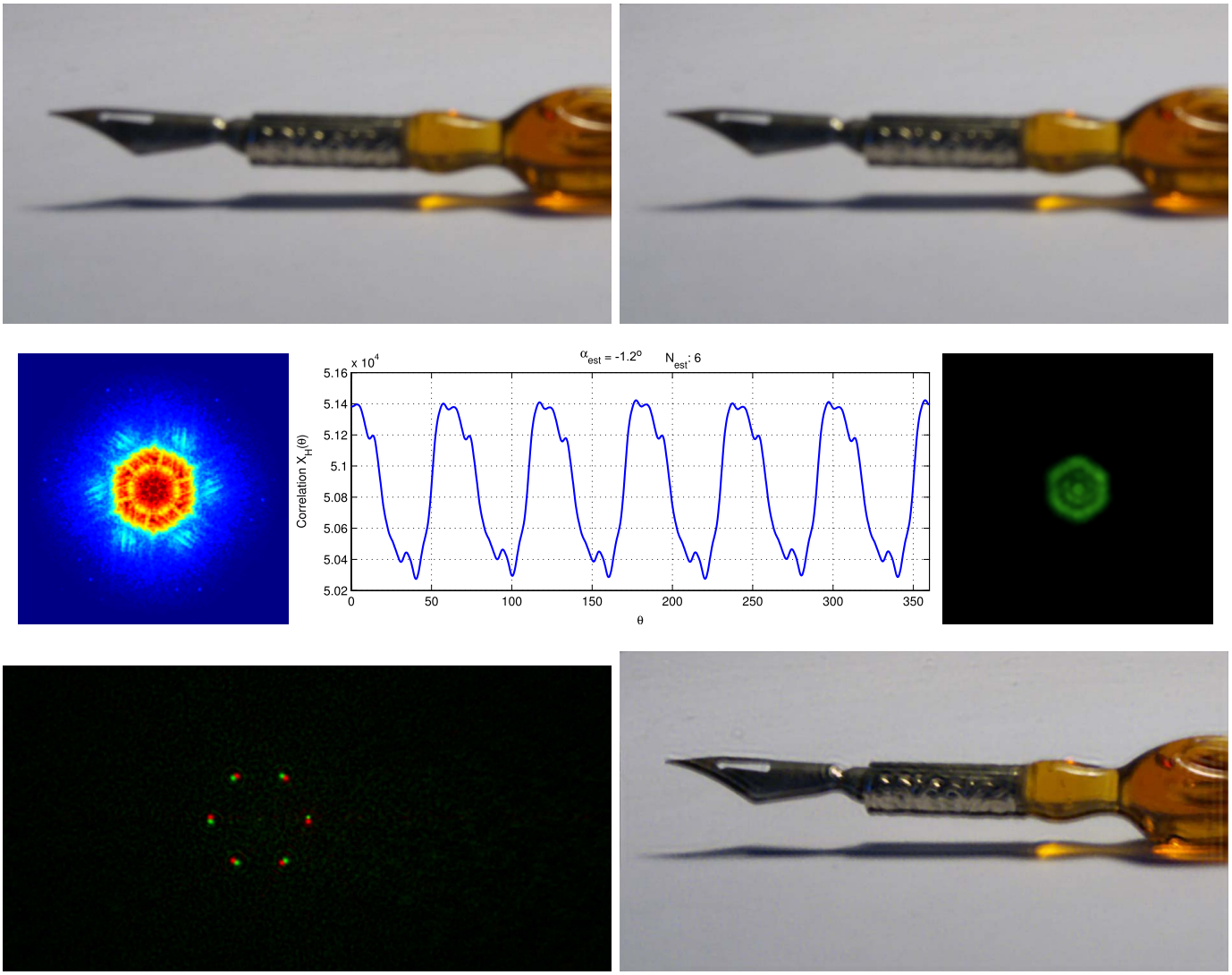

Fig. 12. Two images taken with different focus settings using a hand-held camera *(top row)*. The quantity $|H|$ produced by the PSF axis estimation algorithm in Eq. 16, and the corresponding circular cross-correlation $X_H(\theta)$. The estimated α of the PSF was $-1.2°$. The parameter N was estimated using the algorithm in Section VI *(middle row, left and center)*. The true PSF of the camera, obtained by taking a photo to a bright green point source in a dark environment *(middle row, right)*. Spectral patterns yielded by our registration algorithm, where the red part represents the dihedral peaks $\mathcal{F}^{-1}\{B_j\}$ *(bottom left)*. Result of multichannel blind deconvolution *(bottom right)*.

where one image was relatively sharp but noisy, and the other image was virtually noise-free but out-of-focus. The noisy images had a SNR of approximately 15dB, while the blurred images were taken with a higher exposure time. An example of two images used in this experiment is found in Fig. 8. We used $N = 6$ and obtained 31.4% and 20.3% of misregistrations using respectively the method in [11] and the proposed one.

One of the challenging problems in image registration is a registration of almost periodic scenes. All registration algorithms should be tested under such conditions. Using a hand-held camera (Panasonic Lumix DMC-LX3) we took two shots of a tablecloth with a few safety matches. We manually changed the focus settings to obtain blur, and panned the camera to simulate translation. Since the camera was hand-held, some amount of spurious perspective transformation is also present. We used our algorithm ($N = 6$) to register the images, and estimated the symmetry axis of the PSF using (19). Although the spectral patterns now contain more than one circle, the fitting algorithm found the correct one and the shift parameters were recovered accurately, as can be checked by the positions of the safety matches. We also tried to register these images by a SIFT-based technique [12], which is a popular local registration method. However, SIFT failed completely because of the blur in the sensed image (the sensitivity of SIFT-based registration to image blur was already reported in [11]). The result of this experiment is shown in Fig. 9.

We tested our method also in real situations, where both blur and noise were introduced by the camera settings, and the assumed acquisition model (1) was valid only approximately or locally, and the symmetry of the PSF was not perfectly N-fold. Here we present the results of an experiment, where we took a short video of a static 3D scene by slowly panning the camera. The depth of field of the camera

(Panasonic HC-V700) did not allow both foreground and background to be in focus at the same time. The automatic focus mode of the camera was turned on and the camera always tried to keep the center of the image in focus. Thus the focus settings were automatically re-adjusted when we changed the place we were pointing at. We extracted two frames where the first frame shows the foreground in focus and the background out of focus, and vice-versa for the second frame (see Fig. 11). Bright spots in the scene allows us to estimate the symmetry parameters of the PSF. Clearly, $N = 4$ and one of the symmetry axes is approximately vertical (the estimated angle by means of the algorithm was 4 degrees). As in the previous case, the SIFT-based registration failed due to the blur. Then we used the proposed method of dihedral phase correlation to register these two frames images, and although our method is not specifically designed to handle spatially-varying blur, the result of registration was still accurate. Since we do not know the ground truth, we illustrate the accuracy by performing multifocus fusion (we used the wavelet-based fusion technique [13] for this purpose). The fused product (see Fig. 11) contains only tiny artifacts that are due to the parallax.

Since our method is mostly conceived to be used in conjunction with image fusion algorithms, we also performed an experiment on image deblurring by multichannel blind deconvolution (MBD). In this experiment, two differently blurred photos were taken with a consumer camera (Panasonic Luminx DMC-LX3) to an object that was placed close to the camera lens. The object was so close that, due to the limitations of the optical system, it was not possible to focus the camera on the subject. By keeping the aperture and the exposure time fixed, while manually changing the focus settings between the two shots, we acquired two differently unfocused images (Fig. 12). During the whole process the camera was hand-held; this caused the two images to not be perfectly aligned. The misalignment was mostly composed of a considerable translational component. We estimated the parameters of the PSF: the degree of symmetry N, and the symmetry axis orientation α, by using respectively the algorithms described in Sections V-VI. The estimated parameters were $N = 6$ and $\alpha = -1.2°$. We then used the proposed method to register the two images. The 12 spectral peaks produced by our method appear relatively sharp and reliable, and they are visible in Fig. 12. We utilized the registered pair of images as input to a MBD algorithm (we used the approach described in [14], but our registration algorithm is independent of the particular deconvolution method and can be used as a pre-processing step for any method of this kind). The resulting deblurred image and the estimated PSFs are shown in Fig. 12.

In order to assess the accuracy of our algorithm for the estimation of N, we performed an additional experiment in which we took 100 pairs of images, where the second image of each pair was a translated, blurred, and noisy version of the first image. The procedure used to obtain the images was the same as the one used for the first experiment described in this section. The overlap was fixed to 50%, the PSF's had size 31×31 pixels, and the true N for each image was randomly chosen among $\{3, \ldots, 8\}$ (PSF's with higher values of N would have been approximately circular). The noise levels were $\sigma = 0, 2, 4, 6, 8, 10, 12, 14, 16, 18, 20$ (with pixel gray levels within the range $[0, 255]$). We used (21) to estimate N and we counted the number of images for which we obtained a correct estimate $N_{est} = N$. The results are summarized in Fig. 10.

VIII. Conclusion

In this paper we extended the theory of blur-invariant image registration introduced recently in [11]. While the original method considered only N-fold rotational symmetric blurring functions, here we proposed an analogous technique for dihedral blurs. Although the original method can be employed in case of dihedral blurs as well, the new version contributes to better registration performance as was demonstrated by experiments.

The new method is based on the assumption that the symmetry axis of the PSF is known. This parameter appears explicitly in the definition of the reflection operator. In certain applications this should not be a serious problem because we can measure the camera settings. For those cases where such assumption might be too restrictive, we proposed a simple algorithm of estimation of the symmetry axis of the PSF. It is demonstrated that the use of the axis estimation algorithm has only a minimal impact in terms of registration accuracy when compared to the ideal case of known PSF axis.

The method tolerates small errors in the axis orientation but as the error increases, the method loses its advantage and its performance converges to the performance of the original method from [11].

Generalizations of our method to handle also rotation and scaling are possible in an analogous way to how it was done in traditional phase correlation [8], i.e. by mapping the FT magnitudes into log-polar domain, in which the rotation and scaling are converted to shifts, and rotational symmetry of the PSF is converted to translational symmetry. One could then define projection operators w.r.t. translational symmetry and proceed analogously to the presented method. However, if the axis orientation is unknown, it must be estimated in advance as in the current version.

Acknowledgments

The authors would like to thank Dr. Filip Šroubek for providing the code for multichannel blind deconvolution.

References

[1] B. Zitová and J. Flusser, "Image registration methods: A survey," *Image Vis. Comput.*, vol. 21, no. 11, pp. 977–1000, 2003.

[2] J. Flusser and T. Suk, "Degraded image analysis: An invariant approach," *IEEE Trans. Pattern Anal. Mach. Intell.*, vol. 20, no. 6, pp. 590–603, Jun. 1998.

[3] Y. Bentoutou, N. Taleb, M. Chikr El Mezouar, M. Taleb, and J. Jetto, "An invariant approach for image registration in digital subtraction angiography," *Pattern Recognit.*, vol. 35, no. 12, pp. 2853–2865, 2002.

[4] I. Makaremi and M. Ahmadi, "Wavelet-domain blur invariants for image analysis," *IEEE Trans. Image Process.*, vol. 21, no. 3, pp. 996–1006, Mar. 2012.

[5] Y. Bentoutou, N. Taleb, K. Kpalma, and J. Ronsin, "An automatic image registration for applications in remote sensing," *IEEE Trans. Geosci. Remote Sens.*, vol. 43, no. 9, pp. 2127–2137, Sep. 2005.
[6] J. Flusser, J. Boldyš, and B. Zitová, "Moment forms invariant to rotation and blur in arbitrary number of dimensions," *IEEE Trans. Pattern Anal. Mach. Intell.*, vol. 25, no. 2, pp. 234–246, Feb. 2003.
[7] B. Chen, H. Shu, H. Zhang, G. Coatrieux, L. Luo, and J. L. Coatrieux, "Combined invariants to similarity transformation and to blur using orthogonal Zernike moments," *IEEE Trans. Image Process.*, vol. 20, no. 2, pp. 345–360, Feb. 2011.
[8] E. De Castro and C. Morandi, "Registration of translated and rotated images using finite Fourier transforms," *IEEE Trans. Pattern Anal. Mach. Intell.*, vol. PAMI-9, no. 5, pp. 700–703, Sep. 1987.
[9] V. Ojansivu and J. Heikkilä, "Image registration using blur-invariant phase correlation," *IEEE Signal Process. Lett.*, vol. 14, no. 7, pp. 449–452, Jul. 2007.
[10] S. Tang, Y. Wang, and Y.-W. Chen, "Blur invariant phase correlation in X-ray digital subtraction angiography," in *Proc. IEEE/ICME Int. Conf. Complex Med. Eng.*, May 2007, pp. 1715–1719.
[11] M. Pedone, J. Flusser, and J. Heikkila, "Blur invariant translational image registration for *N*-fold symmetric blurs," *IEEE Trans. Image Process.*, vol. 22, no. 9, pp. 3676–3689, Sep. 2013.
[12] D. G. Lowe, "Distinctive image features from scale-invariant keypoints," *Int. J. Comput. Vis.*, vol. 60, no. 2, pp. 91–110, 2004.
[13] F. Šroubek, S. Gabarda, R. Redondo, S. Fischer, and G. Cristobal, "Multifocus fusion with oriented windows," *Proc. SPIE, Bioeng. Bioinspired Syst. II*, vol. 5839, pp. 264–273, Jun. 2005.
[14] F. Šroubek and J. Flusser, "Multichannel blind deconvolution of spatially misaligned images," *IEEE Trans. Image Process.*, vol. 14, no. 7, pp. 874–883, Jul. 2005.

Matteo Pedone received the M.Sc. degree in computer science from the Sapienza University of Rome, Rome, Italy, in 2007. He is currently pursuing the Ph.D. degree with the Center for Machine Vision Research, University of Oulu, Oulu, Finland. His research interests include computer vision, computational photography, statistical signal processing, differential geometry, and Clifford algebra.

Jan Flusser (M'93–SM'03) received the M.Sc. degree in mathematical engineering from Czech Technical University, Prague, Czech Republic, in 1985, the Ph.D. degree in computer science from the Czechoslovak Academy of Sciences, Prague, in 1990, and the D.Sc. degree in technical cybernetics, in 2001. Since 1985, he has been with the Institute of Information Theory and Automation, Czech Academy of Sciences, Prague. From 1995 to 2007, he was the Head of the Department of Image Processing. Since 2007, he has been the Director of the Institute of Information Theory and Automation. He is a Full Professor of Computer Science with Czech Technical University and Charles University, Prague, where he gives undergraduate and graduate courses in digital image processing, pattern recognition, and moment invariants and wavelets. His research interest covers in moments and moment invariants, image registration, image fusion, multichannel blind deconvolution, and super-resolution imaging. He has authored or co-authored over 150 research publications, including the monograph entitled *Moments and Moment Invariants in Pattern Recognition* (Wiley, 2009), tutorials, and invited/keynote talks at major international conferences. In 2007, he received the award of the Chairman of the Czech Science Foundation for the best research project and the Prize of the Academy of Sciences of the Czech Republic for the contribution to image fusion theory. He was a recipient of the prestigious SCOPUS 1000 Award by Elsevier in 2010.

Janne Heikkilä (SM'15) received the Dr.Techn. degree in information engineering from the University of Oulu, Oulu, Finland, in 1998, where he is currently a Professor of Information Technology with the Department of Computer Science and Engineering, and the Associate Leader of the Center for Machine Vision Research. He has served on committees of several international conferences and as a reviewer in many scientific journals. He is an Associate Editor of *IET Computer Vision* and a member of the Governing Board of the International Association for Pattern Recognition. From 2006 to 2009, he was the President of the Pattern Recognition Society of Finland. His research interests include computer vision, pattern recognition, digital image and video processing, and statistical signal processing. He has contributed to more than 130 peer-reviewed international scientific articles.